Multiport Square Law Detectors: Responsivity Matrix Model and Direct Determination of the Optimum Injection Regime

Philippe Artillan, Ignacio Íñiguez-De-La-Torre, Gaudencio Paz-Martínez, Edouard Rochefeuille, Sergio García-Sánchez, Tomás González, Javier Mateos

▶ **To cite this version:**

Philippe Artillan, Ignacio Íñiguez-De-La-Torre, Gaudencio Paz-Martínez, Edouard Rochefeuille, Sergio García-Sánchez, et al.. Multiport Square Law Detectors: Responsivity Matrix Model and Direct Determination of the Optimum Injection Regime. IEEE Transactions on Microwave Theory and Techniques, 2024, 72 (10), pp.6044 - 6048. 10.1109/TMTT.2024.3390834 . hal-04712776

HAL Id: hal-04712776
https://hal.science/hal-04712776v1

Submitted on 10 Oct 2024

HAL is a multi-disciplinary open access archive for the deposit and dissemination of scientific research documents, whether they are published or not. The documents may come from teaching and research institutions in France or abroad, or from public or private research centers.

L'archive ouverte pluridisciplinaire **HAL**, est destinée au dépôt et à la diffusion de documents scientifiques de niveau recherche, publiés ou non, émanant des établissements d'enseignement et de recherche français ou étrangers, des laboratoires publics ou privés.

Multiport Square Law Detectors: Responsivity Matrix Model and Direct Determination of the Optimum Injection Regime

Philippe Artillan, Ignacio Íñiguez-de-la-Torre, Gaudencio Paz-Martínez, Edouard Rochefeuille, Sergio García-Sánchez, Tomás González, *Senior Member, IEEE*, and Javier Mateos, *Member, IEEE*

***Abstract*—A generic matrix model for the responsivity of millimeter wave (mmW) and sub-THz square law detectors is proposed. The model is valid for any number of ports and takes the biasing conditions into account, the power distribution, the phase-shifts between ports and the frequency dependence of the detector response. The proposed approach is experimentally validated up to 67 GHz on an AlGaN/GaN High Electron Mobility Transistor (HEMT). It could however be used for other types of detectors, including diodes and CMOS detectors. In addition, a reliable mathematical method is presented, allowing the direct determination of the maximum attainable responsivity and the associated optimum excitation. This method avoids a computing time consuming evaluation of the above quantities by constrained optimization, and thus provides an efficient way to evaluate the performances of a square law detector only based on its DC and S-parameters characterization.**

***Index Terms*—CMOS detector, High Electron Mobility Transistor (HEMT) detector, responsivity, square law detector, sub-Thz detection, zero-bias detector**

I. Introduction

SQUARE LAW DETECTORS can be described as biased RF multiports which, due to their nonlinear behavior, provide a large variation in DC measured current or voltage on one port when RF power is applied [1]. Classical RF/THz detection is performed with a one-port detector, being the Schottky barrier diode the most widespread architecture [2]. The choice of a detector is based on numerous figures of merit including operation frequency range (or bandwith), maximum accepted RF power, noise equivalent power, switching speed, *etc*. Many other technologies are studied to provide solutions for specific applications [3]. For sub-THz detection, self-switching diodes seem to be quite promising [4]. Two-port devices such as field effect transistors (HEMTs or MOSFETs) could also be good options thanks to their high level of nonlinearity [5]. However, an adequate engineering process must be performed on the biasing conditions and the coupling between ports to reach maximum responsivity. Empirical models for the responsivity of two-port square law detectors have first been developed in quasi-static regime [6], [7], [8], then extended to high frequency regime using a linear small signal equivalent circuit [9] or directly exploiting S-parameters [10]. All these models are only valid for single port excitation, although some improvement is suggested by exciting gate and drain in anti-phase [11], [12]. The non linear response can however be enhanced by choosing the right excitation with specific power distribution and phase-shift between terminals.

The main goal of this paper is then to provide a matrix model of the responsivity, generalized to any number of ports and to any kind of excitation. Furthermore, a mathematical method based on matrix diagonalization is proposed to directly determine the optimum excitation for maximum responsivity.

We propose in Section II a generalized matrix formulation based on the knowledge (by measurement or simulation) of the scattering parameters and the DC curves of the n-port device under test (DUT). Alternatively, the model may be based just on the knowledge of the scattering parameters under several biasing conditions, thus including additional frequency-dependent information in the calculated parameters. Section III provides an experimental validation of the model in the case of a two-port (GaN-based AlGaN/GaN HEMT) up to 67 GHz and for various magnitude and phase input signals. Section IV presents a methodology based on eigenvalues extraction to directly determine the optimum excitation of the detector to achieve the maximum responsivity, thus avoiding a time consuming constrained optimization of a quadratic form. Finally, conclusions are provided in Section V.

The proposed model is able to provide an accurate determination of the responsivity of the devices without the need for fitting parameters. Moreover, the simplicity of the approach allows its implementation without any modification of the standard measurement protocols of the devices. Finally, the possibility to directly determine the best power injection regime for optimum responsivity can be used to drastically accelerate the design process of square law multiport detectors.

Manuscript received 26 November 2023; revised 15 March 2024; accepted 12 April 2024. Date of publication 29 April 2024; date of current version 7 October 2024. This work was supported in part by MCIN/AEI/10.13039/501100011033 under Grant PID2020-115842RB-I00.

(Corresponding author: Philippe Artillan)

P. Artillan and E. Rochefeuille are with Univ. Grenoble Alpes, Univ. Savoie Mont Blanc, CNRS, Grenoble INP, CROMA (Centre de radiofréquences, optique et micro-nanoélectronique des Alpes), 38000 Grenoble, France (e-mail: philippe.artillan@univ-smb.fr, edouard.rochefeuille@univ-smb.fr).

I. Íñiguez-de-la-Torre, G. Paz-Martínez, S. García-Sánchez, T. González and J. Mateos and are with the Applied Physics Department, and USAL-NANOLAB, Universidad de Salamanca, 37008 Salamanca, Spain (e-mail: indy@usal.es, gaupaz@usal.es, sergio_gs@usal.es, javierm@usal.es, tomasg@usal.es,).

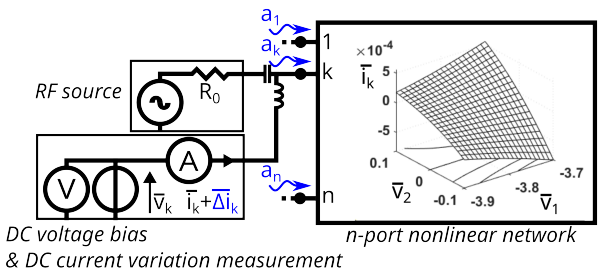

Fig. 1. Generic scheme for RF power detection with an n-port nonlinear device. All ports are voltage biased ($\overline{v_k}$) and excited with an RF source (incident power-wave a_k). The DC bias current $\overline{i_k}$ (when RF power is OFF) is shifted by the DC detection current $\Delta i_k(a_1, \cdots, a_n)$, which depends on the magnitude and phase of the RF signal injected at each port.

II. Responsivity of an n-port detector

A. General Case: RF Power Injected in All Ports

In the following, time domain variables are lowercase, complex phasors are uppercase (except power-wave vectors of phasors a and b) and DC quantities are overlined lowercase.

We consider here an n-port nonlinear device, in which each port k is biased with a voltage $\overline{v_k}$ and excited with an incident RF power-wave a_k at frequency ω through an access of real characteristic impedance R_0 (see Fig. 1), assumed to be the same in all ports for simplicity (the model can be easily generalized just by considering a different value of R_0 for each port). $\overline{v}_k$ are the components of a single vector of voltage biases $\overline{v}$ and a_k are the components of a single vector of incident power waves a.

At port k, the phasor a_k depends on the incident (or "injected") power P_k^{inc} and on the absolute phase ϕ_k of the excitation:

$$a_k = \sqrt{2P_k^{inc}}e^{j\phi_k}. \tag{1}$$

The total power P_{tot}^{inc} injected in the system is the sum of the powers P_k^{inc} injected at each port k:

$$P_{tot}^{inc} = \sum_{k=1}^{n} P_k^{inc} = \sum_{k=1}^{n} \frac{|a_k|^2}{2} = \frac{1}{2}\|a\|^2. \tag{2}$$

The vector of incident power-waves a applied to the detector creates, at each port, a sine voltage represented by the phasor V_k at frequency ω, and we then define the vector of RF voltage phasors V. Now, V can be retrieved by adding the incident power waves $a = (V + R_0 I)/(2\sqrt{R_0})$ and the reflected power waves $b = (V - R_0 I)/(2\sqrt{R_0})$, where I is the vector RF current. The relationship between a and b is given by the the scattering parameters matrix of the detector $b = Sa$ [13]:

$$V = \sqrt{R_0}(a + b) = \sqrt{R_0}(\mathbb{I} + S)a. \tag{3}$$

where $\mathbb{I}$ is the identity matrix.

The transient voltage excitation vector $v(t)$ is then the sum of the DC voltage bias $\overline{v}$ and the harmonic excitation $v^{\omega}(t)$:

$$v(t) = \overline{v} + \underbrace{\Re(Ve^{j\omega t})}_{v^{\omega}(t)}. \tag{4}$$

Due to the nonlinear behavior of the detector, $v^{\omega}(t)$ creates in turn a current $i_k(t)$ at port k [10], which can be expressed thanks to a multivariable local Taylor expansion of order 2 of the DC characteristic $\overline{i}(\overline{v})$ [1], [7], [14]:

$$i_k(t) \approx \underbrace{\overline{i_k}(\overline{v})}_{\overline{i_k}} + \underbrace{\frac{1}{4}V^*\mathcal{H}^k V}_{\overline{\Delta i_k}} + \underbrace{\Re(Y_k V e^{j\omega t})}_{i_k^{\omega}(t)} + \underbrace{\cdots}_{i_k^{2\omega}(t)} + \cdots \tag{5}$$

where Y_k is row k of the Y-parameters matrix of the device (directly measured or deduced from the measured S-parameters), and $\mathcal{H}^k$ is the Hessian matrix of the DC current characteristic $\overline{i_k}(\overline{v})$ at port k:

$$\mathcal{H}_{ij}^k = \frac{\partial^2 \overline{i_k}(\overline{v})}{\partial \overline{v_i} \partial \overline{v_j}}, \tag{6}$$

or, by analogy with the low-frequency case where $\Re(Y_{kj}) = \frac{\partial \overline{i_k}}{\partial \overline{v_j}}$, frequency-dependent coefficients $\mathcal{H}_{ij}^k(\omega)$ can be empirically defined to be directly computed from the measured Y-parameters:

$$\mathcal{H}_{ij}^k(\omega) = \frac{\partial \Re(Y_{kj}(\omega, \overline{v}))}{\partial \overline{v_i}}. \tag{7}$$

Finally, injecting (3) in the $\overline{\Delta i_k}(a)$ term of (5) and dividing by (2), the expression of the responsivity β_k in units of A/W at port k becomes:

$$\beta_k(a) = \frac{\overline{\Delta i_k}(a)}{P_{tot}^{inc}} \approx \frac{R_0}{2\|a\|^2} a^* (\mathbb{I} + S)^* \mathcal{H}^k (\mathbb{I} + S)\, a. \tag{8}$$

The limitations of the proposed model lie in the following assumptions: (*i*) the RF excitations are single-tone weak-signal excitations, (*ii*) the effective maximum degree of the nonlinearity is 2, (*iii*) the source impedances are identical and real (this limitation could be overtaken but would unnecessarily complicate notations) and (*iv*) the frequency dependence of the responsivity $\beta_k(a)$ is fully captured by the frequency dependence of the scattering matrix $S(\omega, \overline{v})$ in eq. (3) and the frequency dependence of the non-linear equivalent conductances $\Re(Y_{kj})$ of the device in eq. (7). On one hand, eq. (3) actually captures the impedance mismatch between the output impedances of the sources and the device. On the other hand, using eq. (7) instead of eq. (6) empirically captures the memory effect of the device, making the model a Volterra series scheme instead of a Taylor series scheme [15], [16]. Identical results are obtained by both approaches up to a few tens of GHz for standard integrated devices, whereas, the agreement with experimental results is significantly improved by using eq. (7) above that frequency limit. It is interesting to note that only equivalent conductances are involved because the non-linear equivalent susceptances $\Im(Y_{kj})$ have no impact on the generation of DC current by rectification.

B. Particular Cases: RF Power Injected in One Single Port

The expression (8) is valid for a diode (only one port with any excitation a_1):

$$\beta^{diode} = \beta_1(a_1) \approx \frac{R_0}{2}\mathcal{H}_{11}^{(k=1)}|1 + S_{11}|^2. \tag{9}$$

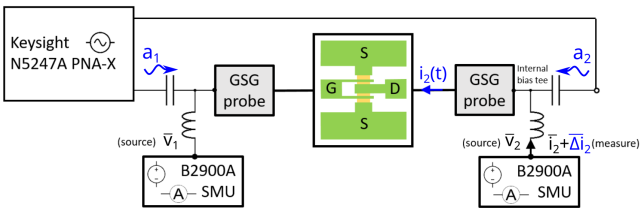

Fig. 2. Schematic drawing of the setup for DC, S-parameters and responsivity characterization. In this setup, the VNA operates as the RF source. The RF power is injected both in the gate and in the drain (thanks to true mode stimulus option), with chosen total incident power and phase-shift. The two-channel SMU biases in voltage the drain and gate terminals of the transistor. Two internal bias-tees allow to couple DC and RF signals. The drain current is measured as detection output. Ground-signal-ground (GSG) probes are used to contact the 50 Ω coplanar waveguide accesses.

In the case of a two port FET such as a HEMT, the expression of the current responsivity at drain port in the case of gate injection (GI) β^{GI} can also be derived from (8). The detection port is the drain ($k = 2$) and the power is fully injected through the gate (port 1), so that $a = (a_1, 0)$, thus with no impact of the phase. These conditions lead to:

$$\beta^{GI} = \beta_2(a_1, 0) \approx \frac{R_0}{2}\left(\mathcal{H}_{11}^{(k=2)}\left|1+S_{11}\right|^2 + \mathcal{H}_{22}^{(k=2)}\left|S_{21}\right|^2 + 2\mathcal{H}_{12}^{(k=2)}\Re[S_{21}^*(1+S_{11})]\right). \tag{10}$$

Finally, the expression of the current responsivity at drain port in the case of drain injection (DI) β^{DI} can again be derived from (8) with $k = 2$ and $a = (0, a_2)$:

$$\beta^{DI} = \beta_2(0, a_2) \approx \frac{R_0}{2}\left(\mathcal{H}_{11}^{(k=2)}\left|S_{12}\right|^2 + \mathcal{H}_{22}^{(k=2)}\left|1+S_{22}\right|^2 + 2\mathcal{H}_{12}^{(k=2)}\Re[S_{12}^*(1+S_{22})]\right). \tag{11}$$

It is to be noted that expressions (10) and (11) have been already obtained in [10].

III. Experimental Validation in the Case of a Two-Port

A. Experimental Setup

In order to validate the above presented theory, the case of a two-port is studied further. The experimental setup is sketched in Fig. 2, where a two-channel Keysight B2902A SMU and Keysight N5247A PNA-X are used for the measurements. First, the DC curves are measured. Then, the S-parameters at each bias point are obtained. Port 1 corresponds to the gate and port 2 to the drain, and the calibration planes are brought to the transistors terminals thanks to a Short-Open-Load-Thru calibration. Finally, the VNA is employed as an RF source. Power signals from 100 MHz to 67 GHz are injected into the transistor simultaneously through both the drain and the gate terminals. The coupled signals have been generated using the S93460B True-Mode Stimulus option that allows to control the phase-shift and power distribution. The losses due to the cables, connectors and probes have been adequately compensated [6]. The SMU averages the output DC rectified current at the drain port, thus providing the current responsivity $\beta(a)$ in A/W. Everything is controlled with a home-made Matlab code.

B. Variables Definition

The vector of RF power-wave phasors a contains two components a_1 and a_2. With a total power budget of $2P_{tot}^{inc}$ and an arbitrary null phase for a_1 with no loss of generality, one can define $0 \leq \theta \leq 180°$ and $-180 \leq \phi \leq 180°$ to respectively represent the proportion of power fed into port 2 compared to port 1, and the phase-shift between the two ports. The excitation vector a is then defined as:

$$a = (a_1, a_2) = \sqrt{2P_{tot}^{inc}}\left(\cos\left(\frac{\theta}{2}\right), \sin\left(\frac{\theta}{2}\right)e^{j\phi}\right). \tag{12}$$

Equivalently, the total power P_{tot}^{inc} and the angles θ and ϕ can be retrieved from vector a by the following relations:

$$\begin{cases} P_{tot}^{inc} = \frac{|a_1|^2+|a_2|^2}{2}, \\ \theta = 2\arctan\left(\left|\frac{a_2}{a_1}\right|\right), \\ \phi = \arg\left(\frac{a_2}{a_1}\right). \end{cases} \tag{13}$$

C. Experimental Measurements

An AlGaN/GaN HEMT with $L_g = 75$ nm gate length, $W = 2 \times 25$ μm gate width has been employed as a test vehicle. Precisely, it is the very same transistor already characterized in [10]. The responsivity $\beta(\theta, \phi)$ has been measured and modeled at a voltage bias of $(\overline{v_1}, \overline{v_2}) = (-3.8\ V, 0\ V)$. The total injected power is always $P_{totdB}^{inc} = -20$ dBm. Fig. 3(a) shows the results at 1 GHz. At this frequency, the model (8) gives the same results whatever the computation of the Hessian matrix is made from the DC curves using (6) or from the Y parameters using (7), and the latter is presented here. The phase-shift ϕ has obviously no impact in the two cases of single port excitation (gate injection when $\theta = 0°$ and drain injection when $\theta = 180°$). On the contrary, it is of great importance in all other combined excitation cases. The extrema of responsivity are obtained around $\phi \approx 0°$ or $180°$ and close to $\theta \approx 90°$ that corresponds to equally distributed injected power between gate and drain. Finally, the agreement between the model and the experimental results is really good. Fig. 3(b) shows the results at 67 GHz. In such a high frequency case, the Hessian matrix computed from the Y-parameters at 67 GHz gives better results and are presented here. The agreement is also very acceptable, thus validating the model up to 67 GHz.

IV. Direct Determination of the Ideal Excitation for Maximum Responsivity

A. Optimum RF Excitation for Maximum Responsivity

The proposed model allows the computation of the responsivity $\beta(a, \overline{v}, \omega)$ as a function of the magnitude and phase of the incident power on each port, the voltage biases and the frequency. The objective of this section is to maximize the

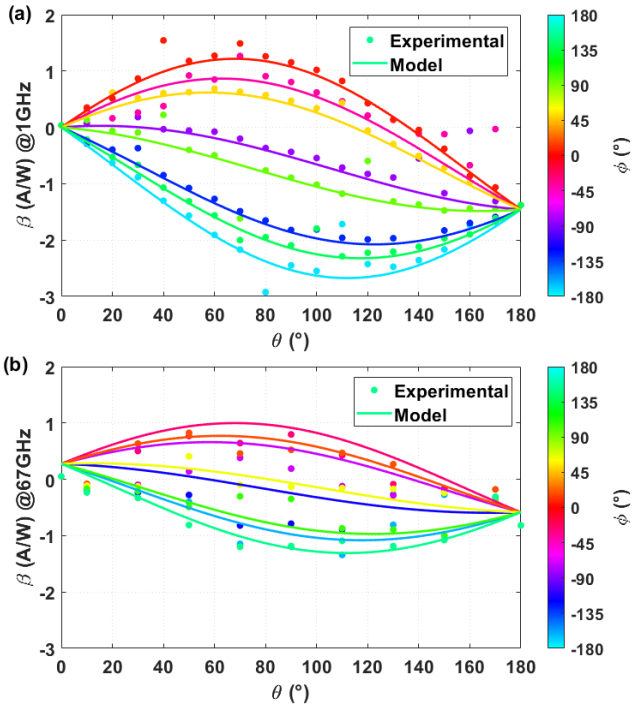

Fig. 3. Responsivity $\beta(\theta,\phi)$ of a HEMT at (a) 1 GHz and (b) 67 GHz. Confrontation of the responsivity modeled by (8) (lines) with the responsivity measured in True Mode Stimulus (dots).

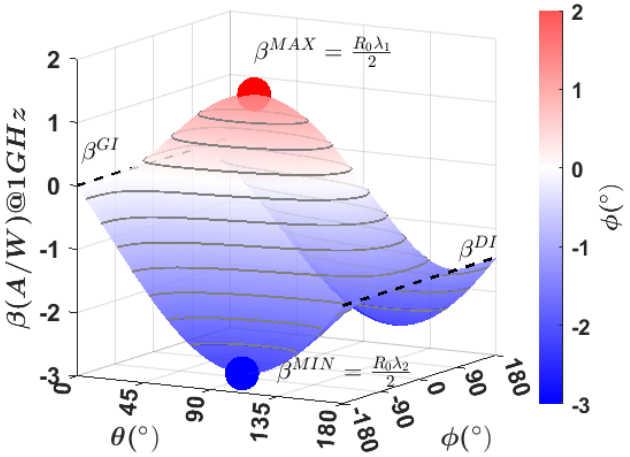

Fig. 4. $\beta(\theta,\phi)$ at $\overline{v_1}$ =-3.8 V, $\overline{v_2}$ =0 V, $\frac{\omega}{2\pi}$ =1 GHz computed using the model described by (8) under the constrain of $P^{inc}_{totdB} = -20$ dBm. Note that $\theta = 0°$ (GI, gate injection regime) and $\theta = 180°$ (DI, drain injection regime) are independent of the phase-shift ϕ. The red point β^{MAX} and the blue point β^{MIN} have been computed by the direct determination method based on the eigen basis using (18).

responsivity $\beta_k(a)$ of (8) by optimizing magnitudes and phases of every component of the power injection vector a, under the constraint of injecting a chosen amount of total power $P^{inc}_{tot} = \frac{1}{2}\|a\|^2$ [*i.e.* a must verify (2)]. Defining

$$H \widehat{=} (\mathbb{I}+S)^* \mathcal{H}^k (\mathbb{I}+S), \tag{14}$$

equation (8) can be rewritten as:

$$\beta_k(a) \approx \frac{R_0}{2\|a\|^2} a^* H a. \tag{15}$$

Since $\mathcal{H}^k$ is the Hessian matrix of a real function, it is real and symmetric, and H is then a Hermitian matrix ($H = H^*$). The finite-dimensional spectral theorem [17], [18] states that H is unitarily diagonalizable with real eigenvalues. One can then find n real eigenvalues λ_i (let's assume that $\lambda_1 \geq \lambda_2 \geq \cdots \geq \lambda_n$) and n orthonormal eigenvectors $\hat{e}_i$ so that:

$$H\hat{e}_i = \lambda_i \hat{e}_i. \tag{16}$$

As $\hat{e}_i$ are orthonormal vectors, $\hat{\mathcal{B}} = \{\hat{e}_1, \hat{e}_2, \cdots, \hat{e}_n\}$ is an orthonormal basis of C^n, *i.e.* $< \hat{e}_i, \hat{e}_j >= \hat{e}_i^* \hat{e}_j = \delta_{ij}$. One can express a on the eigenbasis $\hat{\mathcal{B}}$:

$$a = \sum_{i=1}^{n} \hat{a}_i \hat{e}_i. \tag{17}$$

Injecting (16) and (17) in (15) leads to:

$$\beta_k(a) \approx \frac{R_0}{2\|a\|^2} \sum_{i=1}^{n} |\hat{a}_i|^2 \lambda_i. \tag{18}$$

Finally, since λ_1 (*resp.* λ_n) is the highest (*resp.* lowest) eigenvalue, the maximum (*resp.* minimum) achievable value of β_k is obtained when $a = \hat{e}_1$ (*resp.* $\hat{e}_n$):

$$\beta^{MAX}_k = \beta_k(\hat{e}_1) = \frac{R_0\lambda_1}{2}, \tag{19}$$

$$\beta^{MIN}_k = \beta_k(\hat{e}_n) = \frac{R_0\lambda_n}{2}. \tag{20}$$

Note than depending on the signs and values of λ_1 and λ_n, the optimum (maximum absolute value) responsivity may be β^{MAX}_k or β^{MIN}_k. Thus, knowing the eigenvalues and eigenvectors of H, it is possible to determine the optimum responsivity and the corresponding power distribution conditions in relative amplitude and phase for any n-port square law detector. It is to mention that the expressions of β^{MAX}_k and β^{MIN}_k do not depend on the total injected power because the detector operates in its linear region of responsivity (in A/W). Fig. 4 illustrates this direct determination of β^{MAX} and β^{MIN} in the case of the same GaN HEMT studied in Section III-C. Note that in this case the optimum value is β^{MIN}. We remark that the agreement of the extreme values extracted directly by eq. (18) is excellent with those identified in the complete map calculated using (8), as well as with the experimental values in Fig. 3(a), with the great advantage that the computing time is much shorter.

B. Optimum Voltage Biases for Maximum Maximorum Responsivity

The fast computation of the optimum RF power excitation a presented in section IV-A allows to compute β^{MAX} and β^{MIN} versus bias voltages. Fig. 5 represents such computations and also represents the corresponding GI (gate injection) and DI (drain injection) regimes. One can verify that both those single port excitation regimes are in between the

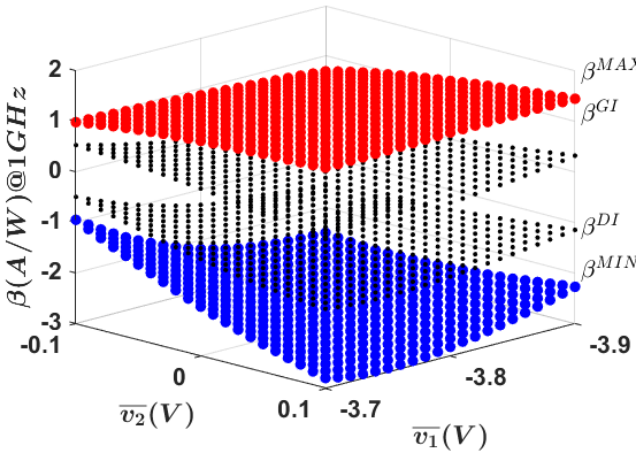

Fig. 5. Maximum, minimum, GI and DI responsivities $\beta(\overline{v_1}, \overline{v_2})$ at 1 GHz and $P^{inc}_{totdB} = -20$ dBm.

computed extrema, thus indicating that an adequate power repartition engineering leads to responsivity improvement.

V. Conclusion

A generalized model of the responsivity of an n-port device is proposed. Thanks to the model, the maximum responsivity for a given frequency can be computed and the associated excitation is provided in terms of bias conditions, power distribution and phase-shift between the ports. The model has been experimentally validated for a two-port GaN HEMT with very good agreement up to 67 GHz. The optimum responsivity is obtained for a 0° or 180° phase-shift and a specific power distribution between gate and drain, allowing an increase of the responsivity by almost a factor 2 compared to standard single port excitation.

References

[1] A. Cowley and H. Sorensen, "Quantitative comparison of solid-state microwave detectors," *IEEE Trans. Microw. Theory Techn.*, vol. 14, no. 12, pp. 588–602, Dec. 1966.

[2] J. L. Hesler and T. W. Crowe, "NEP and responsivity of THz zero-bias Schottky diode detectors," in *2007 Joint 32nd Int. Conf. on Infrared and Millimeter Waves and the 15th Int. Conf. on Terahertz Electronics*. IEEE, 2007, pp. 844–845.

[3] E. Javadi, D. B. But, K. Ikamas, J. Zdanevičius, W. Knap, and A. Lisauskas, "Sensitivity of field-effect transistor-based terahertz detectors," *Sensors*, vol. 21, no. 9, p. 2909, 2021.

[4] I. Íñiguez-de-la Torre, E. Pérez-Martín, P. Artillan, E. Rochefeuille, H. Sánchez-Martín, G. Paz-Martínez, T. González, and J. Mateos, "Current and voltage responsivity up to 110 GHz in GaN asymmetric nano-diodes," *Applied Physics Letters*, vol. 123, no. 12, p. 123503, 09 2023.

[5] F. Aniel, G. Auton, D. Cumming, M. Feiginov, S. Gebert, T. González, C. Li, A. Lisauskas, H. Marinchio, J. Mateos, C. Palermo, A. Song, J. Treuttel, L. Varani, and N. Zerounian. "Terahertz electronic devices," in Springer Handbook of Semiconductor Devices, edited by M. Rudan , R. Brunetti , and S. Reggiani (Springer, 2023).

[6] S. Kim, D.-W. Park, K.-Y. Choi, and S.-G. Lee, "MOSFET characteristics for terahertz detector application from on-wafer measurement," *IEEE Trans. Terahertz Sci. Technol.*, vol. 5, no. 6, pp. 1068–1077, Nov. 2015.

[7] M. I. W. Khan, S. Kim, D.-W. Park, H.-J. Kim, S.-K. Han, and S.-G. Lee, "Nonlinear analysis of nonresonant THz response of MOSFET and implementation of a high-responsivity cross-coupled THz detector," *IEEE Trans. Terahertz Sci. Technol.*, vol. 8, no. 1, pp. 108–120, Jan. 2018.

[8] G. Paz-Martínez, I. Íñiguez-de-la Torre, H. Sánchez-Martín, T. González, and J. Mateos, "Analysis of GaN-based HEMTs operating as RF detectors over a wide temperature range," *IEEE Trans. Microw. Theory Techn.*, vol. 71, no. 7, pp. 3126–3135, 2023.

[9] M. A. Andersson and J. Stake, "An accurate empirical model based on volterra series for FET power detectors," *IEEE Trans. Microw. Theory Techn.*, vol. 64, no. 5, pp. 1431–1441, May 2016.

[10] G. Paz-Martínez, P. Artillan, J. Mateos, E. Rochefeuille, T. González, and I. Íñiguez-de-la Torre, "A closed-form expression for the frequency dependent microwave responsivity of transistors based on the I-V curve and S-Parameters," *IEEE Trans. Microw. Theory Techn.*, 2023.

[11] X. Yang, A. Vorobiev, K. Jeppson, and J. Stake, "Describing broadband terahertz response of graphene FET detectors by a classical model," *IEEE Transactions on Terahertz Science and Technology*, vol. 10, no. 2, pp. 158–166, 2020.

[12] A. H. Mahi, H. Marinchio, C. Palermo, A. Belghachi, and L. Varani, "Enhanced thz detection through phase-controlled current response in field-effect transistors," *IEEE Electron Device Letters*, vol. 34, no. 6, pp. 795–797, 2013.

[13] K. Kurokawa, "Power waves and the scattering matrix," *IEEE Trans. Microw. Theory Techn.*, vol. 13, no. 2, pp. 194–202, 1965.

[14] X. Zhang, J. Grajal, J. L. Vazquez-Roy, U. Radhakrishna, X. Wang, W. Chern, L. Zhou, Y. Lin, P.-C. Shen, X. Ji *et al.*, "Two-dimensional mos2-enabled flexible rectenna for wi-fi-band wireless energy harvesting," *Nature*, vol. 566, no. 7744, pp. 368–372, 2019.

[15] J. J. Bussgang, L. Ehrman, and J. W. Graham, "Analysis of nonlinear systems with multiple inputs," *Proceedings of the IEEE*, vol. 62, no. 8, pp. 1088–1119, 1974.

[16] S. Maas, *Nonlinear Microwave and RF Circuits, Second Edition*. IEEE Press, 2003.

[17] S. Axler, *Operators on Inner Product Spaces. In: Linear Algebra Done Right. Undergraduate Texts in Mathematics.* Springer, 2015. [Online]. Available: https://doi.org/10.1007/978-3-319-11080-6_7

[18] B. Hall, *The Spectral Theorem for Bounded Self-Adjoint Operators: Statements. In: Quantum Theory for Mathematicians. Graduate Texts in Mathematics*. Springer, New York, NY, 2013, vol. 267. [Online]. Available: https://doi.org/10.1007/978-1-4614-7116-5_7